

reduce the temperature to prevent power degradation or damage to the solar panel. With this, the author creates a prototype entitled "Prototype Photovoltaic Charger Controller Based on Proportional-Integral-Derivative (PID) with Overheat Protection System."

2. LITERATURE REVIEW

2.1. Solar Panel

Solar cells, silicon-based semiconductor devices, operate based on the principle of converting light energy into electrical energy. The interaction between solar photons and the silicon crystal structure results in the splitting of electron-hole pairs. The p-type and n-type semiconductor layers connected form a p-n junction, creating an internal electric field. When photons are absorbed, electrons are excited throughout the p-n junction, producing an electric current. The energy conversion efficiency of solar cells is greatly influenced by the properties of the semiconductor, cell structure, and the intensity and spectrum of solar radiation.



Figure 1. Solar Panel

2.2. Battery

Batteries in solar cell systems act as electrical energy storage. The reversible electrochemical process allows batteries to convert electrical energy into chemical energy during charging and vice versa, into electrical energy during discharging. The redox reactions that occur at the electrodes and electrolytes are the basis of this energy conversion process. Secondary batteries, which can be recharged many times, are commonly used in solar cell systems because of their efficiency and flexibility.

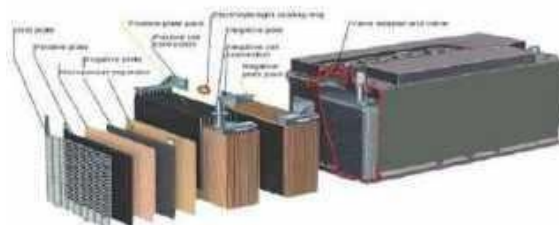


Figure 2. Solar Cell Battery Construction

2.3. Buck-Boost Converter

A buck-boost DC-DC converter has the unique ability to produce an output voltage that is either higher or lower than the input voltage. The working principle involves the periodic opening and closing of the switch, which causes the inductor current to rise and fall alternately. The average value of the output voltage can then be adjusted by manipulating the ratio of the switch on and off times (duty cycle). When the duty cycle is more than 0.5, the converter operates in boost mode, increasing the input voltage. Conversely, if the duty cycle is less than 0.5, the converter operates in buck mode, decreasing the input voltage, Triyono.B & Prasetyo, (2019).



Figure 3. Buck Boost Converter

2.4. INA 219 Sensor

The INA219 sensor is an electronic device designed to measure voltage and electric current in DC circuits by utilizing the Hall effect principle. This device is equipped with an I2C interface that allows digital communication with a microcontroller. INA219 is capable of measuring currents up to $\pm 3.2\text{A}$ with a resolution of up to 0.8mA . In addition, this sensor can also measure shunt voltages up to 26V . Accurate and precise measurement capabilities make the INA219 an ideal choice for power monitoring applications in renewable energy systems and power distribution systems, Maiti.A & Das.S, (2020).



Figure 3. Sensor INA219

2.5. DHT11 Sensor

The DHT11 sensor is a digital sensor module designed to measure temperature and relative humidity. The working principle of this sensor is based on changes in the resistance of the resistive element along with changes in temperature and humidity. The analog data obtained is then converted into a digital signal via an internal ADC before being sent to the microcontroller. The main advantages of the DHT11 lie in its high response speed, good accuracy, and ease of use. The calibration coefficients stored in the OTP memory ensure consistent measurement results, Rumalutur,S & Mappa, A (2019).



Figure 5. DHT11 Sensor

2.6. Arduino Ano

Arduino Uno R3 is a popular microcontroller development board based on the ATmega328 microcontroller. Equipped with 14 digital I/O pins, 6 analog pins, and 32 KB of flash memory, the Arduino Uno R3 provides a flexible platform for various electronics projects. Its USB interface facilitates the software development process through the Arduino IDE. The presence of various types of shields and additional modules further enriches the functionality of this board. This study shows that Arduino Uno R3 is an effective and efficient tool for learning and developing embedded systems, Mujahid, A. & Hashim, U (2020).



Figure 6. Arduino Uno

2.7. DC Water Pump

A DC (Direct Current) water pump is a pump that is powered by direct current electricity, usually from a limited power source such as a battery or solar panel. This pump is more efficient in energy use than an AC water pump because it does not require an inverter to convert alternating current to direct current. In addition, DC water pumps can operate at low voltages, making them ideal for off-grid applications and in remote, hard-to-reach locations.



Figure 7. DC Water Pump

2.8. Liquid Crystal Display (LCD)

(LCD) 16x2 is a display component commonly used in microcontroller systems. With the ability to display alphanumeric characters and special symbols, LCD plays an important role as a user interface to display information such as sensor measurement results, text, and menus. Flexibility in 4-bit or 8-bit configurations, as well as programmable character generator features, make 16x2 LCD a popular choice in various applications, including embedded systems and Arduino projects, Yusuf, M & Isnawaty, R.R. (2016).

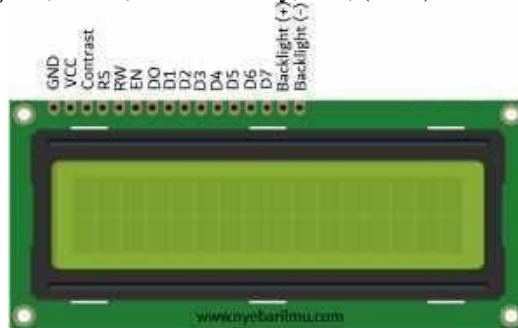


Figure 8. Liquid Crystal Display (LCD)

2.9. PID Control

PID control has been widely used in industry, covering almost 90% of its use, Gunawan, I, Akbar, T & Ilham, M.G (2020). Its popularity is due to the simplicity of this control system and its ability to provide excellent results when set properly. PID consists of three control actions: proportional (K_p), integral (K_i), and derivative (K_d).

Each action in PID control has a specific function. The proportional action reduces the rise time, thereby reducing the steady-state error. The integral action is responsible for eliminating the steady-state error. However, if only PI is controlled, the transient response can worsen. This is where the derivative action comes in, improving transient responses such as settling time and overshoot. The combination of these three actions in PID control improves system stability, reduces overshoot, and speeds up the transient response.

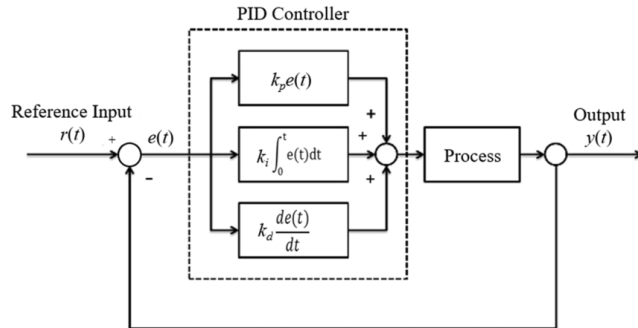


Figure 10. PID Control

3. RESEARCH METHOD

3.1. Research Design

The method used in this study is a descriptive method with a quantitative approach that will be delivered using the ADDIE model.

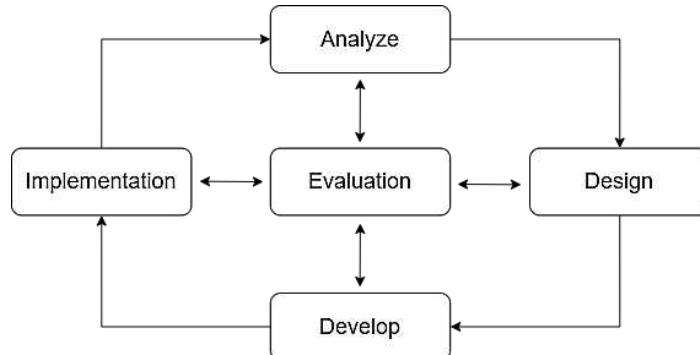


Figure 11. Research Design

3.2. Tool Design

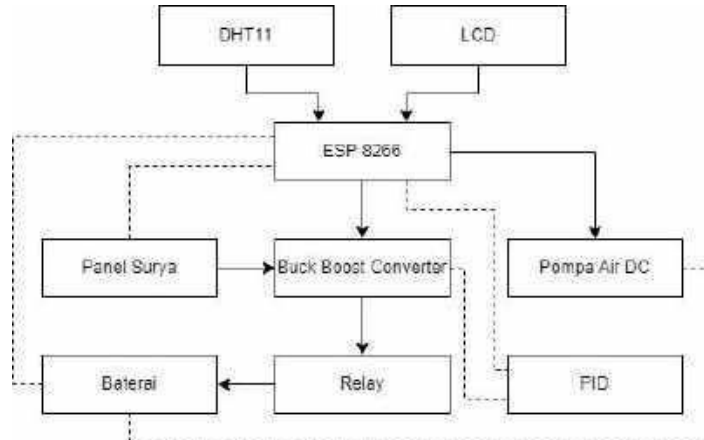


Figure 12. Tool Block Diagram

This tool can later work by increasing or decreasing the voltage according to the set point to produce maximum voltage output and using the PID logic method on the buck-boost converter to optimize battery charging. The following is the flowchart of the tool in this study:

1. Starting the tool system.
2. The INA219 sensor monitors the current and voltage at the output of the solar panel, which will be displayed on the LCD screen.

3. This parameter is used as input for the PID controller to stabilize the battery charging process.
4. PID control determines whether the output voltage is according to the setpoint; if not, the buck-boost converter increases or decreases the output voltage according to the setpoint.

The Overheat Protection System will be active if the temperature on the surface of the solar panel exceeds the limit value, by disconnecting the output from the solar panel and spraying water on its surface so that the temperature drops. Here's how it works:

1. The DHT11 sensor reads the temperature on the surface of the solar panel.
2. The relay disconnects the output flow from the solar panel to the buck-boost converter due to the temperature exceeding the set threshold.
3. Water will be sprayed on the surface of the solar panel by the sprayer

4. RESEARCH RESULTS AND DISCUSSION

4.1. Solar Panel Testing

The author uses a 20 WP Solar Panel. This component is the main object that will be the generator to charge the battery voltage and receive the cooling system work process.



Figure 13. Solar Panel Test

Table 1. Solar Panel Test Results

Time	Voltage Output (V)	Arus Output (A)
07.00-08.00	17,4	1,79
12.00-13.00	20,52	1,8
16.00-17.00	18,8	1,76

Analysis Results Obtained:

In the solar panel testing that was carried out, measurements were obtained as in the table above. By carrying out the measurements, the author can determine the magnitude of the voltage and current that can be obtained from the solar panel output. So it can be concluded that the higher the light intensity, the greater the voltage that will be produced. In the experiment, the highest voltage data was obtained, namely 20.52V at 12.00-13.00, and the lowest 17.4V at 07.00-08.00. From this experiment, it can be concluded that in one day the 20 WP solar panel can produce a voltage of 20 V with normal bright conditions.

4.2. INA 219 Sensor Testing

The INA 219 Sensor Testing must be carried out to find out whether the installed sensor is working according to its function or not. This test is important because a sensor that is not functioning properly can cause errors in

measurement and data analysis. The test was carried out using a hair dryer as a tool to provide a heat load on the system, thus allowing verification of the accuracy of current and voltage measurements by the INA219 sensor.

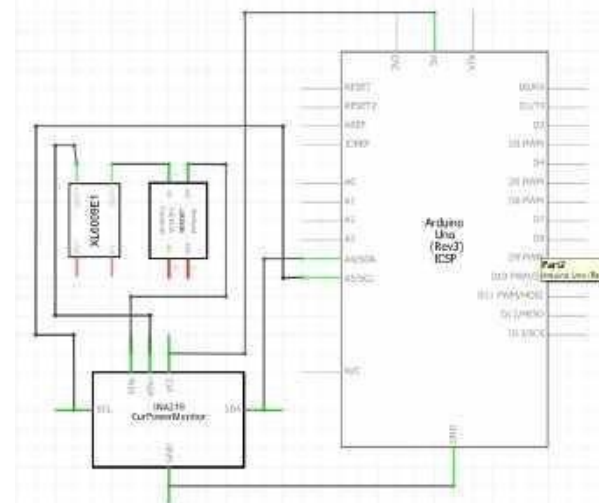


Figure 14. Sensor INA219 Circuit

Table 2. Sensor INA219 Test Results

No.	Measurement (V)	appearance LCD (V)	difference (V)	Error (%)
1	14,28	13,2	1,08	7,5
2	13,47	13,26	0,21	1,5
3	12,65	12,43	0,22	1,7
4	13,68	13,0	0,68	4,9
5	13,34	13,0	0,34	2,5
Mean			0,45	3,2

The results of the analysis obtained:

Based on the table above, the sensor can read the voltage magnitude. From the data, the results of the INA219 sensor test are compared with the measuring instrument so that the average voltage error is 3.2%. So that the accuracy of the INA219 sensor is 96.7%.

4.3. DHT11 Temperature Sensor Testing

The DHT11 Sensor Testing is carried out by placing the temperature sensor behind the solar panel. To obtain an accurate temperature value on the solar panel on the DH11 sensor, compare the temperature value on the thermogun.

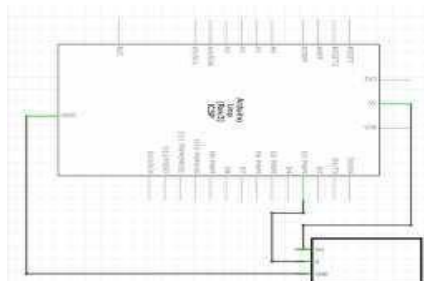


Figure 15. DHT11 Temperature Sensor Circuit

Table 3. Temperature Measurement Results

No.	Measurement (V)	appearance LCD (V)	difference (V)	Error (%)
1	37,9 ⁰ C	37,4 ⁰ C	0,5	1,3
2	40,1 ⁰ C	39,7 ⁰ C	0,4	0,9
3	36,0 ⁰ C	35,8 ⁰ C	0,2	0,6
Mean			0,9	2,8

4.4. Overheat Protection System Testing

The overheat protection system testing on solar panels is to ensure that it can detect excessive temperatures and automatically activate the cooling mechanism to prevent damage to the panels.



Figure 16. Overheat Protection System Test

Table 4 . Overheat Protection System Test Results

o'clock	Set Point Temperature	Time	Temp start	Temp end
07.00-09.00	35 ⁰	39s	37 ⁰	34 ⁰
	35 ⁰	34s	36 ⁰	33 ⁰
	35 ⁰	33s	35 ⁰	33 ⁰
	35 ⁰	32s	34 ⁰	34 ⁰
	35 ⁰	10s	36 ⁰	34 ⁰
11.00-13.00	35 ⁰	40s	40 ⁰	33 ⁰
	35 ⁰	42s	39 ⁰	34 ⁰
	35 ⁰	45s	38 ⁰	32 ⁰
	35 ⁰	37s	37 ⁰	32 ⁰
	35 ⁰	32s	36 ⁰	33 ⁰
	35 ⁰	5s	35 ⁰	34 ⁰
	35 ⁰	0s	34 ⁰	34 ⁰

o'clock	Set Point Temperature	Time	Temp start	Temp end
15.00-17.00	350	0s	330	330
	350	0s	320	320
	350	0s	320	320

4.5. PID Testing

PID Control works by calculating the error value by comparing the actual output value with the desired value.

$$\text{Error value} = \text{actual value} - \text{setpoint value}$$

After obtaining the error value, the controller will try to minimize the error value at all times by adjusting the control variables that can be changed to kp, ki, and kd values. The PID controller will calculate the output based on the difference between the current temperature (process variable) and the desired temperature (setpoint). The output of the PID is a value that usually regulates the speed or intensity of the control, but in this case, the author will use it to control the duration of the pump on/off time.



Figure 17. PID Program

In the program above, the PID controller calculates the error value as the difference between the setpoint and the actual value. In this project, the PID system that is set is the value of Kp, Ki, and Kd of:

Kp: 1

Ki: 1

Kd: 1

Based on these coefficients, the image above shows the results of the system analysis carried out with PID control based on these coefficients. From the results of the buck boost converter test, determine the error in the PID using the following formula.

Error = Voltage - Set Point

P = Kp x Error

I = Ki x (Total Error + Past Error)

D = Kd x (Error - Past Error)

PID = P + I + D

Overshoot = Timer Stable / Set Point Voltage x 100%

Table 5. PID Test Results

No.	Timer Stabil	voltage (V)	current (A)	Set Point voltage (V)	Error	P	I	D
morning								
1	3s	13,3V	1,8A	13V	0,3	0,3	0,3	0,3
2	8s	13,7V	1,65A	13V	0,7	0,7	1	0,4

3	5s	13,4V	1,73A	13V	0,4	0,4	1,4	-0,3
4	7s	13,6V	1,58A	13V	0,6	0,6	2	0,2
5	4s	13,5V	1,69A	13V	0,5	0,5	2,5	-0,1
Afternoon								
1	3s	13,2V	1,92A	13V	0,2	0,2	0,2	0,2
2	12s	13,9V	1,68A	13V	0,9	0,9	1,1	0,7
3	8s	13,8V	1,84A	13V	0,8	0,8	1,9	-0,1
4	5s	13,6V	1,78A	13V	0,6	0,6	2,5	-0,2
5	6s	13,5V	1,63A	13V	0,5	0,5	3	-0,1
Evening								
1	7s	13,4V	1,87A	13V	0,4	0,4	0,4	0,4
2	9s	13,6V	1,71A	13V	0,6	0,6	1	0,2
3	10s	13,5V	1,65A	13V	0,5	0,5	1,5	-0,1
4	6s	13,3V	1,85A	13V	0,3	0,3	1,8	-0,2
5	2s	13,2V	1,86A	13V	0,2	0,2	2	-0,1

Based on the table and graph data above, it can be determined:

Morning Test Overshoot = $8s/60 = 0.14/13 \times 100\% = 0.0107\%$ Afternoon Test Overshoot = $12s/60 = 0.2/13 \times 100\% = 0.015\%$ Evening Test Overshoot = $10s/60 = 0.17/13 \times 100\% = 0.013\%$.

The results of the analysis obtained:

In this test, the PID system control error can be determined, and the highest voltage results in the morning are 13.7V with a setpoint of 13V with an overshoot of 0.0107%, during the day it is 13.9V with an overshoot of 0.015%, and in the afternoon it is 13.6V with an overshoot of 0.013%.

4.6. Overall System Testing

After testing each component or device, both hardware and software, the next step is to test the overall system. This test was conducted to determine the work results of the Prototype Photovoltaic Charger Controller Based on a Proportional-Integral-Derivative (PID) with Overheat Protection System.



Figure 17. Overall System Testing

Overall system testing is carried out after each component has been successfully tested and is by its function. This tool begins by initiating the system. The INA219 sensor then monitors the output voltage of the buck-boost converter and displays the values on the 16x2 LCD screen. This parameter then becomes input for the PID controller, which is tasked with stabilizing the battery charging process. The PID control will determine whether the output voltage is by the specified setpoint. If not, the buck-boost converter will adjust the output voltage by increasing or decreasing it according to the set point.

The overheat protection system will be active if the temperature on the surface of the solar panel exceeds the set limit. The DHT11 sensor will read the temperature on the surface of the solar panel. When the temperature exceeds the specified limit, the relay will disconnect the output from the buck-boost converter to the system components. At the same time, the water pump will turn on and pump water to the sprayer. Water will then be sprayed onto the surface of the solar panel by the sprayer to lower the temperature.

5. CONCLUSION AND RECOMMENDATIONS

5.1. Conclusion

Based on the experiments and discussions, it can be concluded that:

1. This Final Project tool uses a PID controller with parameters Kp, Ki, and Kd each of 1, to regulate the voltage on the buck-boost converter. The voltage setpoint is set at 13 V, with data updates every 300 ms, and the PWM output is set in the range of 0 to 250. This system works by increasing the PWM output if the output voltage is lower than the setpoint, then what the system will do is reduce the PWM output so that the output voltage is higher than the setpoint. The goal is to stabilize the fluctuating output voltage of the solar panel so that battery charging is more efficient and the battery lifetime can last longer.
2. Based on the experiments conducted, the regulation of the stability of the buck-boost converter output voltage for the battery charger using the PID method shows quite good performance with a relatively small overshoot. In the morning, the highest voltage recorded was 13.7V with a setpoint of 13V and an overshoot of only 0.0107%. During the day, the voltage increases to 13.9V with an overshoot of 0.015%, while in the afternoon, the voltage decreases slightly to 13.6V with an overshoot of 0.013%.

5.2. Recommendations

During the process of making this tool, the author identified several shortcomings that affected performance. To improve the quality and functionality of the tool in the future, the following suggestions are given:

1. Current stabilizer components need to be integrated to prevent current surges when there is a voltage drop, ensuring system stability and security.
2. The Internet of Things (IoT) can be implemented to provide benefits such as remote monitoring and control of the system, as well as increased efficiency through real-time data collection and automation.

REFERENCES

- [1] Alnavis, N. B., Wirawan, R. R., Solihah, K. I., & Nugroho, V. H. (2024). Energi listrik berkelanjutan: potensi dan tantangan penyediaan energi listrik di Indonesia. *Journal of Innovation Materials, Energy, and Sustainable Engineering*, 1(2). <https://doi.org/10.61511/jimese.v1i2.2024.544>
- [2] Azmi, U., Sasongko, N. A., Murtiana, S., & Saputro, G. E. (2024). The Evaluation of Use Photovoltaics (PV) in Renewable Energy Technology as Sustainability Strategies. *International Journal of Humanities Education and Social Sciences*. <https://doi.org/10.55227/ijhess.v4i1.1207>
- [3] Bashiru, O., Ochem, C., Enyejo, L. A., Nkula Manuel, H. N., & Adeoye, T. O. (2024). The crucial role of renewable energy in achieving the sustainable development goals for cleaner energy. *Global Journal of Engineering and Technology Advances*, 19(3), 011–036. <https://doi.org/10.30574/gjeta.2024.19.3.0099>
- [4] F, F., & Muhammad, F. (2022). Optimization of Renewable Energy in Indonesian Energy Mix 2025. *Global Conference on Business and Social Sciences Proceeding*, 14(2), 1. [https://doi.org/10.35609/gcbssproceeding.2022.2\(59\)](https://doi.org/10.35609/gcbssproceeding.2022.2(59))
- [5] Gunawan, I., Akbar, T., & Ilham, M. G. (2020). Prototipe penerapan Internet of Things (Iot) pada monitoring level air tandon menggunakan nodemcu Esp8266 dan Blynk. Infotek: *Jurnal Informatika dan Teknologi*, 3(1), 1-7.
- [6] Maiti, A., & Das, S. (2020). A high-precision power monitoring system based on INA219 sensor. *Journal of Electrical Engineering & Technology*, 15(3), 1059- 1066. <https://doi.org/10.1007/s42835-020-00057-5>
- [7] Mujahid, A., & Hashim, U. (2020). Arduino-based embedded system design for educational applications. *IEEE Access*, 8, 114368-114377. <https://doi.org/10.1109/ACCESS.2020.3005686>
- [8] Raihan, A. (2023). *An overview of the energy segment of Indonesia: present situation, prospects, and forthcoming advancements in renewable energy technology*. <https://doi.org/10.56556/jtie.v2i3.599>
- [9] Rumalutur, S., & Mappa, A. (2019). Temperature and Humidity Moisture Monitoring System with Arduino R3 and DHT 11. *Electro Luceat*, 5(2), 40- 47.
- [10] Triyono, B., Prasetyo, Y., Winarno, B., & Wicaksono, H. H. (2021, March). Electrical Motor Interference Monitoring Based On Current Characteristics. In *Journal of Physics: Conference Series* (Vol. 1845, No. 1, p. 012044). IOP Publishing.
- [11] Yusuf, M., & Isnawaty, R. R. (2016). Implementasi Robot Line Follower Penyiram Tanaman Otomatis Menggunakan Metode Proportional–Integral–Derivative Controller (PID). *Jurnal semanTIK*, 2(1).